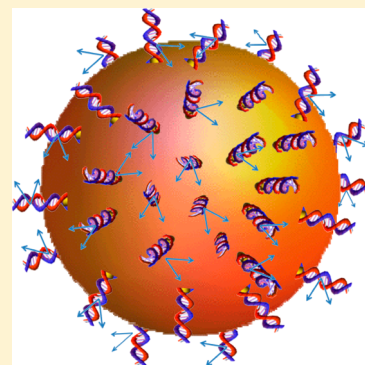


Probing the Relative Orientation of Molecules Bound to DNA by Second-Harmonic Generation

Jerry Icban Dadap^{*,†} and Kenneth B. Eisenthal[‡]Departments of [†]Applied Physics and Applied Mathematics and [‡]Chemistry, Columbia University, New York, New York 10027, United States

S Supporting Information

ABSTRACT: We develop a model to probe the relative orientation of two second-order polarizable daunomycin molecules that are intercalated into a DNA duplex using optical second-harmonic (SH) generation. The SH field generated by the daunomycin molecules interfere with each other. Because the interference depends on the relative orientation of the daunomycin molecules, we can control the interference by changing the number of base pairs separating them. The relative orientation changes as the number of base pairs separating them, multiplied by 36° , which is the twist angle between neighboring base pairs. In this paper, we derive a set of relationships between the relative angle of the molecules and the nonlinear susceptibility elements, and we calculate the SH field generated by the DNA/molecular-pair complex attached to an isotropic dielectric sphere. Calculations reveal that the SH intensity varies periodically with the relative orientation of the two chromophores in the plane perpendicular to the helical axis. The predicted periodicity is in close agreement with experimental results. Structural changes induced by foreign molecules binding to DNA will change the relative orientation of the two chromophores and thereby change the SH interference pattern. We discuss the potential of this SH interference method in providing a new way to probe structural changes induced by the formation of biomolecule complexes. An important feature of the method is that it is label-free, that is, the binding molecule, in this case, daunomycin, is not tagged.



INTRODUCTION

In a recent study, the relative spatial orientation of two molecules bound to a DNA duplex was systematically controlled and subsequently probed by second-harmonic (SH) generation (SHG).¹ This study reveals that the SH intensity depended on the relative angle Φ between two molecules. With the exception of a small Φ -independent contribution, the SH signal was found to be proportional to $(1 + \cos \Phi)$. This observation provides a tantalizing scheme for the use of SHG as a solution-phase “molecular protractor”. In particular, it has been determined that a daunomycin molecule intercalates at specific recognition sites of the DNA helix² with its aromatic plane oriented at right-angles to the axis of the DNA helix.³ Thus, one daunomycin molecule was rotated relative to another by changing the number of base pairs separating them on a given DNA duplex that was attached to a colloidal silica microparticle (see Figure 1).¹ In going up or down each “rung”, that is, a base pair, of the helical DNA “ladder”, the daunomycin chromophore is rotated by 36° , which is the twist angle of the DNA helix.⁴ Thus, the relative angle Φ between two molecules separated by n base pairs is $\Phi \approx 36^\circ n$.

To explain the specific SH signal dependence on Φ , which is also the angle between the induced second-order dipole moments $\mathbf{p}_A^{(2)}$ and $\mathbf{p}_B^{(2)}$ (see Figure 1, inset), a simple SHG model was previously employed in which each of the resulting SH fields $\mathbf{E}_A^{(2\omega)}$ and $\mathbf{E}_B^{(2\omega)}$, is aligned along $\mathbf{p}_A^{(2)}$ and $\mathbf{p}_B^{(2)}$,

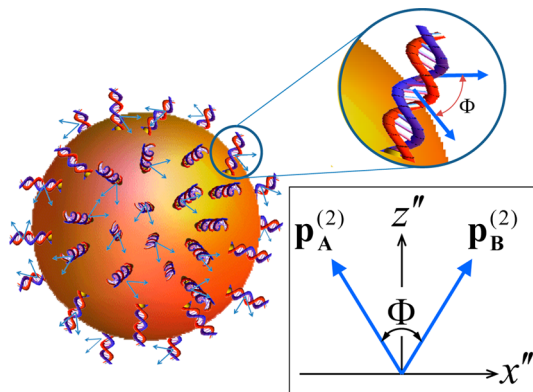


Figure 1. Schematic depiction of DNA duplexes affixed on a spherical particle. The relative orientation of two intercalating nonlinear polarizable molecules (denoted as arrows) bound to each DNA indicate the directions of the induced SH dipole moments. Inset: Schematic representation of the induced SH dipole moments $\mathbf{p}_A^{(2)}$ and $\mathbf{p}_B^{(2)}$ of two identical molecules, A and B, respectively, in the molecular-pair principal coordinate system defined by (x'', y'', z'') with relative orientation angle Φ .

Received: August 3, 2014

Revised: October 29, 2014

respectively.¹ If the two fields have the same magnitude and phase, the resulting SH intensity is proportional to $|\mathbf{E}_A^{(2\omega)} + \mathbf{E}_B^{(2\omega)}|^2 = 2|\mathbf{E}_A^{(2\omega)}|^2 (1 + \cos \Phi)$, in agreement with the experimental findings, except for an additional contribution from a background signal that is independent of Φ . This model, however, does not take into account the relationship between the incident field, $\mathbf{E}^{(\omega)} = \mathbf{E}_0^{(\omega)} e^{i\mathbf{k}\cdot\mathbf{r}}$, and the generated SH electric field $\mathbf{E}^{(2\omega)} = \mathbf{E}_0^{(2\omega)} e^{i\mathbf{K}\cdot\mathbf{r}}$, where $\mathbf{E}_0^{(\omega)}$ and $\mathbf{E}_0^{(2\omega)}$ are the field amplitudes, \mathbf{k} and \mathbf{K} are the wave vectors of the fundamental and SH fields, respectively, and \mathbf{r} is the position vector.

We assume that the dipole moments $\mathbf{p}_A^{(2)}$ and $\mathbf{p}_B^{(2)}$ lie in the $x''z''$ plane, where the double-prime coordinates refer to the molecular frame, and are oriented symmetrically relative to the z'' axis (Figure 1 inset). The $(1 + \cos \Phi)$ -dependence of the signal is obtained provided that the phases and amplitudes of $\mathbf{E}_A^{(2\omega)}$ and $\mathbf{E}_B^{(2\omega)}$ are equal, which can be achieved only under the condition in which the amplitude of the fundamental field $\mathbf{E}_0^{(\omega)}$ is along the molecular $y''z''$ plane, except when $\mathbf{E}_0^{(\omega)}$ is along y'' , wherein there is no induced SH polarization because the incident field would be orthogonal to the in-plane transition moments of the daunomycin molecules. However, this situation is rarely satisfied because of the random orientation of the molecular pair relative to the local surface, which is equivalent to the condition of in-plane isotropy of our system. Thus, a more exact treatment is necessary in order to explain the observed dependence of the SH signal with the relative orientation Φ .

In this paper, we consider the equivalent problem of calculating the nonlinear optical response of nonlinear polarizable molecular pairs that are randomly oriented on an arbitrary surface; the two molecules within each pair are oriented relative to each other by the angle Φ . We then obtain the associated SH field and radiation patterns from these molecular pairs that are randomly distributed on the surface of a spherical particle. To that end, we carry out the following three steps: (1) We first determine the effective hyperpolarizability $\alpha^{(2)}$ of a single molecular pair; (2) we then extract the surface nonlinear susceptibility $\chi_s^{(2)}$ associated with this effective hyperpolarizability for a collection of these molecular pairs on a surface; and finally, (3) we calculate the surface-generated SH electric field for a spherical particle having the surface nonlinear susceptibility obtained in step (2).

THEORY

Calculation of Effective Hyperpolarizability $\alpha^{(2)}$ of the Molecular Pair. We begin by considering two identical molecules A and B, schematically shown as arrows in Figure 1, inset, each having a rod-like second-order nonlinear optical polarizability $\beta_{\nu\nu\nu}^{(2)}$ where ν is the local axis of the induced SH dipole moment of each molecule. For purposes of calculation of the effective nonlinear optical response, we assume that the molecules are spatially overlapped and that the overall nonlinear response is dependent only on the relative molecular orientation since the typical distance L between the two molecules is of the order of a few Ångströms to a few nanometers, which is determined by the number of base-pair separation between them; hence, the phase associated with this length scale is negligible, that is, $\sim L/\lambda \ll 1$, where λ is the wavelength of the fundamental beam. We neglect local-field effects and further assume that the molecules are noninteracting so that each of the molecule's hyperpolarizability is unchanged by the presence of the other.

In the first step, as described above, we calculate the effective hyperpolarizability $\alpha^{(2)}$ of the pair of nonlinear-active chromophores. The resulting surface nonlinear susceptibility $\chi_s^{(2)}$ will be the same regardless of the chosen coordinate system used in calculating $\alpha^{(2)}$. Thus, for simplicity, we arbitrarily chose a coordinate system (x'', y'', z'') of the molecular pair such that the molecular pair, schematically denoted by the induced second-order dipole moments $\mathbf{p}_A^{(2)}$ and $\mathbf{p}_B^{(2)}$, lies in the $x''z''$ plane and placed symmetrically, as indicated in the inset of Figure 1 (see also Figure 2a). This coordinate system is one

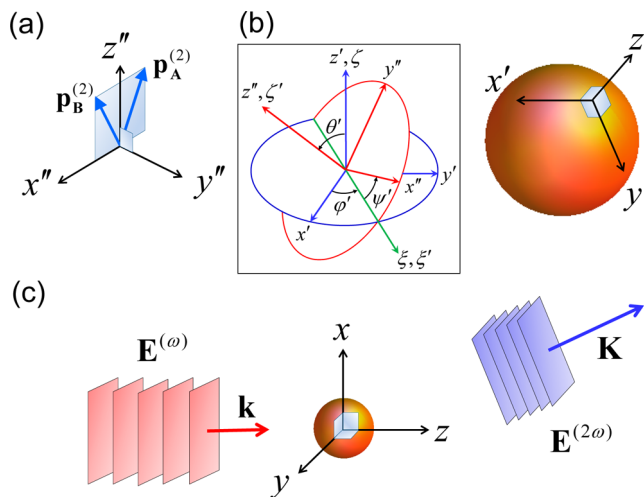


Figure 2. Coordinate systems used in the calculations: (a) Principal axes (x'', y'', z'') of the molecular pair. (b) Local-surface reference frame (x', y', z') . Inset: Euler transformation between reference frames (x', y', z') and (x'', y'', z'') . (c) Laboratory reference frame (x, y, z) showing plane waves corresponding to the fundamental and SH electric fields, $\mathbf{E}^{(\omega)}$ and $\mathbf{E}^{(2\omega)}$, respectively, with their corresponding wave vectors \mathbf{k} and \mathbf{K} .

possible reference frame that yields the smallest number of effective hyperpolarizability tensor elements $\alpha_{ijk}^{(2)}$ of the molecular pair, that is, the coordinate system corresponds to a set of principal axes of the molecular pair. The fundamental electric field may be written in the molecular-pair reference frame as $\mathbf{E}^{(\omega)} = E_{x''}^{(\omega)} \hat{\mathbf{x}}'' + E_{y''}^{(\omega)} \hat{\mathbf{y}}'' + E_{z''}^{(\omega)} \hat{\mathbf{z}}''$, or more succinctly, $\mathbf{E}^{(\omega)} = \sum_i \hat{\mathbf{e}}_i E_i^{(\omega)}$, where $\hat{\mathbf{e}}_i \equiv \hat{\mathbf{i}}$ is the unit vector along the i -direction and $i = \{x'', y'', z''\}$. The induced SH dipole moments are defined as $\mathbf{p}_A^{(2)} = \hat{\nu}_A \beta_{\nu\nu\nu}^{(2)} (\mathbf{E}^{(\omega)} \cdot \hat{\nu}_A)^2$ and $\mathbf{p}_B^{(2)} = \hat{\nu}_B \beta_{\nu\nu\nu}^{(2)} (\mathbf{E}^{(\omega)} \cdot \hat{\nu}_B)^2$. From the inset of Figure 1, the unit vectors of $\mathbf{p}_{A,B}$ may be expressed as $\hat{\nu}_{A,B} = \mp \sin(\Phi/2) \hat{\mathbf{x}}'' + \cos(\Phi/2) \hat{\mathbf{z}}''$, where the minus and plus signs correspond to the A and B molecules, respectively. Hence, the total second-order dipole moment, $\mathbf{p}^{(2)} = \mathbf{p}_A^{(2)} + \mathbf{p}_B^{(2)}$, becomes

$$\mathbf{p}^{(2)} = 2\beta_{\nu\nu\nu}^{(2)} \cos\left(\frac{\Phi}{2}\right) \left\{ 2 \sin^2\left(\frac{\Phi}{2}\right) E_{x''}^{(\omega)} E_{z''}^{(\omega)} \hat{\mathbf{x}}'' + \left[\sin^2\left(\frac{\Phi}{2}\right) E_{x''}^{(\omega)} E_{x''}^{(\omega)} + \cos^2\left(\frac{\Phi}{2}\right) E_{z''}^{(\omega)} E_{z''}^{(\omega)} \right] \hat{\mathbf{z}}'' \right\} \quad (1)$$

By definition, the SH dipole moment $\mathbf{p}^{(2)}$ is related to the effective hyperpolarizability $\alpha^{(2)}$ according to $\mathbf{p}^{(2)} = \alpha^{(2)} : \mathbf{E}^{(\omega)} \mathbf{E}^{(\omega)}$ or, equivalently,

$$\mathbf{p}^{(2)} = \sum_{i,j,k} \hat{\mathbf{e}}_i \alpha_{ijk}^{(2)} E_j^{(\omega)} E_k^{(\omega)} \quad (2)$$

where $\{i,j,k\} = \{x'',y'',z''\}$. Comparing eqs 1 and 2, we extract the following nonvanishing tensor elements of the effective hyperpolarizability:

$$\alpha_{z''z''z''}^{(2)} = 2\beta_{\nu\nu\nu}^{(2)} \cos^3\left(\frac{\Phi}{2}\right) \quad (3a)$$

$$\alpha_{z''x''x''}^{(2)} = 2\beta_{\nu\nu\nu}^{(2)} \cos\left(\frac{\Phi}{2}\right) \sin^2\left(\frac{\Phi}{2}\right) \quad (3b)$$

$$\alpha_{x''x''x''}^{(2)} = \alpha_{x''z''z''}^{(2)} = 2\beta_{\nu\nu\nu}^{(2)} \cos\left(\frac{\Phi}{2}\right) \sin^2\left(\frac{\Phi}{2}\right) \quad (3c)$$

Note that these nonvanishing components of $\alpha^{(2)}$ correspond to a molecule that exhibits nonlinear response only in the plane of the molecular dipole moments $\mathbf{p}_A^{(2)}$ and $\mathbf{p}_B^{(2)}$. In addition, from eqs 3b and 3c, we find that $\alpha_{z''x''x''}^{(2)} = \alpha_{x''z''z''}^{(2)} = \alpha_{x''x''x''}^{(2)}$, thus indicating that $\alpha^{(2)}$ has only two independent tensor elements.

In the second step, we calculate the nonlinear susceptibility $\chi_s^{(2)}$, which is defined in terms of the local surface coordinates (x',y',z') , as shown in Figure 2b. We assume that the molecular pairs are randomly oriented with respect to the plane that is locally tangential to the surface of the sphere. Thus, the molecule–surface system possesses in-plane isotropy. Since inversion symmetry is broken along the coordinate normal to the surface, SHG is allowed. For the case of SHG, there are at most four independent elements of the nonlinear susceptibility $\chi_s^{(2)}$ in the local-surface reference frame: $\chi_{s,z'z'z'}^{(2)}$, $\chi_{s,z'x'x'}^{(2)} = \chi_{s,x'z'z'}^{(2)}$, $\chi_{s,x'x'x'}^{(2)} = \chi_{s,y'y'y'}^{(2)}$, and $\chi_{s,y'y'z'}^{(2)} = -\chi_{s,y'z'y'}^{(2)}$, and the susceptibility elements are invariant to the permutation of the last two indices arising from the intrinsic permutation symmetry.

Figure 2 displays the progression of the coordinate systems used in our calculations, from the molecular to local-surface to laboratory reference frames. The molecular frame (x'',y'',z'') is related to the local-surface reference frame (x',y',z') through the Euler transformation as shown in the inset of Figure 2b, with the Euler angles $\{\varphi',\theta',\psi'\}$ defined by a sequence of rotations through various coordinate systems $(x',y',z') \rightarrow (\xi,\eta,\zeta) \rightarrow (\xi',\eta',\zeta') \rightarrow (x'',y'',z'')$ via the matrix $\mathbf{A} \equiv \mathbf{A}(\varphi',\theta',\psi') = \mathbf{R}_\zeta(\psi')\mathbf{R}_\xi(\theta')\mathbf{R}_x(\varphi')$, where $\mathbf{R}_i(\sigma)$ is defined as the rotation matrix corresponding to a rotation with respect to axis i by an angle σ . Thus, matrix \mathbf{A} transforms (x',y',z') to (x'',y'',z'') , that is, $x_i'' = \sum_j A_{ij}x_j'$, where A_{ij} is the matrix element of \mathbf{A} . The inverse transformation, which corresponds to the transformation from the molecular frame (x'',y'',z'') to the local-surface frame (x',y',z') is then described by the matrix $\mathbf{T} = \mathbf{A}^{-1}$, that is, $x_i' = \sum_j T_{ij}x_j'' = \sum_j A_{ji}^{-1}x_j''$.

Calculation of Surface Nonlinear Optical Susceptibility $\chi_s^{(2)}$. The surface nonlinear susceptibility $\chi_s^{(2)}$, defined with respect to the local-surface frame (x',y',z') , is related to the hyperpolarizability $\alpha^{(2)}$, defined with respect to the molecular-pair frame (x'',y'',z'') , according to the relation⁵

$$\chi_{s,ijk}^{(2)} = N_s \sum_{a,b,c} \langle T_{ia}T_{jb}T_{kc} \rangle \alpha_{abc}^{(2)} \quad (4)$$

where N_s is the surface density of the molecular pairs and the angular brackets imply orientational averaging. Explicit forms of the resulting four independent $\chi_{s,ijk}^{(2)}$ elements are presented in the Supporting Information for the case of a planar molecule with a plane of mirror symmetry perpendicular to the x'' -axis, at $x'' = 0$, similar to our molecular-pair system.

Substituting eqs 3a–3c into eq 4 and carrying out orientational averaging with the assumption of in-plane

isotropy, we find that the number of independent elements of $\chi_s^{(2)}$ is reduced from four to two: $\chi_{s,\perp\perp\perp}^{(2)}$ and $\chi_{s,\perp\parallel\parallel}^{(2)} = \chi_{s,\parallel\perp\perp}^{(2)} = \chi_{s,\parallel\parallel\parallel}^{(2)}$, given by

$$\begin{aligned} \chi_{s,\perp\perp\perp}^{(2)} &= 2N_s\beta_{\nu\nu\nu}^{(2)} \left[3 \cos\left(\frac{\Phi}{2}\right) \sin^2\left(\frac{\Phi}{2}\right) \langle \cos \theta' \rangle \langle \sin^2 \psi' \rangle \right. \\ &\quad \left. + \cos^3\left(\frac{\Phi}{2}\right) \langle \cos^3 \theta' \rangle \left(1 - 3 \tan^2\left(\frac{\Phi}{2}\right) \langle \sin^2 \psi' \rangle \right) \right] \quad (5a) \end{aligned}$$

$$\begin{aligned} \chi_{s,\perp\parallel\parallel}^{(2)} &= \chi_{s,\parallel\perp\perp}^{(2)} \\ &= N_s\beta_{\nu\nu\nu}^{(2)} \left[\cos\left(\frac{\Phi}{2}\right) \langle \cos \theta' \rangle \left(1 - 3 \sin^2\left(\frac{\Phi}{2}\right) \langle \sin^2 \psi' \rangle \right) \right. \\ &\quad \left. - \cos^3\left(\frac{\Phi}{2}\right) \langle \cos^3 \theta' \rangle \left(1 - 3 \tan^2\left(\frac{\Phi}{2}\right) \langle \sin^2 \psi' \rangle \right) \right] \quad (5b) \end{aligned}$$

where \perp and \parallel indicate the coordinates normal (z') and parallel (x' or y') to the local surface, respectively. The term $\chi_{s,x'y'z'}^{(2)}$ vanishes. In addition, for an arbitrarily oriented molecular pair, we see from eqs 5a and 5b that the resulting elements of $\chi_s^{(2)}$ have a rather complicated dependence on Φ as well as on the orientational moments given by $\langle \cos \theta' \rangle$, $\langle \cos^3 \theta' \rangle$, and $\langle \sin^2 \psi' \rangle$. For the case of our system in which the DNA helical axis is, on average, oriented normal with respect to the surface, the two chromophores intercalate with their planes perpendicular to the DNA helical axis. Consequently, the orientation of the plane of the molecular pair, that is, the $x''z''$ -plane, is approximately parallel to the local surface, and may be described by the Euler angles $\theta' \approx \pi/2$ and $\psi' \approx 0$ (see Figure 2b, inset). It is important to note that if the molecular pairs are exactly aligned along the plane of the surface, corresponding to $\theta' = \pi/2$, the nonlinear susceptibility vanishes as can be seen in eqs 5a and 5b because of isotropic averaging. If we define $\theta' = \pi/2 - \gamma$, where γ is a small angle ($\ll 1$), we can expand eqs 5a and 5b in terms of powers of γ , ψ' , and their products. Keeping the lowest-order contributions of orders $\sim O(\gamma)$ and $\sim O(\psi')$, and neglecting higher-order contributions, for example, $\sim O(\gamma^3)$ or $\sim O(\gamma\psi'^2)$, we find that the leading-order contributions to $\chi_s^{(2)}$ in eqs 5a and 5b are as follows:

$$\chi_{s,\perp\perp\perp}^{(2)} \approx 0 \quad (6a)$$

$$\chi_{s,\perp\parallel\parallel}^{(2)} = \chi_{s,\parallel\perp\perp}^{(2)} \approx N_s \langle \gamma \rangle \beta_{\nu\nu\nu}^{(2)} \cos\left(\frac{\Phi}{2}\right) \quad (6b)$$

Hence, the dominant nonlinear susceptibility elements that contribute to the SH field are $\chi_{s,\perp\parallel\parallel}^{(2)}$ and $\chi_{s,\parallel\perp\perp}^{(2)}$, which have the same magnitude and, more importantly, despite the complex angular dependencies of $\chi_s^{(2)}$ on Φ , as shown in eqs 5a and 5b, the final form of these nonlinear susceptibilities has a simple proportionality with $\cos(\Phi/2)$. The approximately zero value of the $\chi_{s,\perp\perp\perp}^{(2)}$ term reflects the fact that the plane of molecular pair is nearly parallel to the local surface of the particle. Since the SH field $E^{(2\omega)} \propto \chi_s^{(2)}$, it is proportional to $\cos(\Phi/2)$ via eq 6b, and the measured signal is proportional to $\cos^2(\Phi/2) = (1 + \cos \Phi)/2$, in agreement with the experimental results.¹ Furthermore, this SH-signal scaling with $(1 + \cos \Phi)$ is independent of the shape of the substrate, that is, planar substrate or particle surface, provided that the in-plane isotropic

symmetry of the interface holds and the substrate is comprised of isotropic medium.

The use of particles as substrates provides two key advantages over planar substrates: (1) More molecules can be irradiated since the signal can arise from within the focal volume of the laser in contrast to a 2-D array of molecules on a planar surface, and (2) the concentration of DNA molecules can be increased without changing the inter-DNA separation by simply increasing the number of particles, thus, increasing the signal-to-noise ratio. As previously shown,⁶ the total SH signal scales with the density of particles at sufficiently low particle concentration. Care must be taken, however, in increasing the particle concentration since optical effects (e.g., multiple scattering, absorption, etc.) or particle–particle interaction (e.g., aggregation) may become significant. Thus, as a rule of thumb, the particle concentration may be increased provided that the SH signal does not deviate from linearity with the particle density.

Despite the fact that the strict directionality of the SH emission is compromised, such an issue can be mitigated in many ways. Two possible solutions are (1) collecting the signal in all directions, for example, with an integrating sphere, and (2) making use of particles with diameters comparable to or larger than the excitation wavelength, in conjunction with large-numerical-aperture lenses to capture the majority of the SH signal. The latter case arises from the coherent nature of the harmonic-generation process. In particular, despite the expected cancellation from oppositely directed dipole sources in a centrosymmetric object comprised of isotropic medium, the effect of retardation of the electromagnetic waves within the object may prevent perfect cancellation of the total SHG field.^{6–8} For spherical particles of finite size but much smaller than the wavelength λ of the excitation light, the SH signal scales as a^6 and, in addition, the SH field has been found to arise from a combination of a nonlocally excited dipole moment and a locally excited quadrupole moment of comparable amplitudes.⁷ These two lowest-order moments interfere to give rise to distinctive radiation patterns with vanishing signal along the axial direction. As the size of the particle increases, higher-order multipole moments begin to contribute to the SH field such that for achiral sources, the signal remains vanishing along the axial direction but the number of radiation lobes increase and begin to tilt toward the forward-scattering direction.⁹ We will illustrate this case below by calculating the SH radiation pattern arising from the surface of a typical “large” spherical-particle substrate.

Calculation of the SH Field from a Spherical Particle.

In the final step of the calculation, we now consider SHG for the case where the molecular pairs that are intercalated into the DNA helices are uniformly distributed on a spherical particle. We neglect at this stage the contribution from the surface-DNA system since its corresponding SH signal is negligible due to lack of resonance, whereas the signal arising from the daunomycin chromophores is strong due to two-photon resonance enhancement.¹ This contribution together with another possible source due to the polarization of water molecules is considered in the next section.

Because of the small difference in the refractive indices, for example, at $\lambda = 800$ nm, of the particle (silica microsphere, $n \approx 1.43$) and its environment (water, $n \approx 1.34$), we may employ the Rayleigh–Gans–Debye (RGD) approximation^{10–18} to obtain an analytic, closed-form expression for the SH field. Thus, for the general case of a single spherical particle with

isotropic surface, the SH field, under the RGD approximation in the radiation zone at the field point $\mathbf{r}(r, \theta, \varphi)$, may be expressed as

$$\mathbf{E}^{(2\omega)} = \frac{K^2 \exp(iK_1 r) V(E_0^{(\omega)})^2}{r} (\hat{\mathbf{r}} \times \mathbf{p}_{\text{eff}}) \times \hat{\mathbf{r}} \quad (7)$$

where $K_1 = n(2\omega)K$, n is the refractive index of the ambient medium, $K = 2\omega/c$, $V = 4\pi a^3/3$ is the volume of the spherical particle, and \mathbf{p}_{eff} is the effective dipole moment, which is dependent on the effective nonlinear susceptibility elements as well as the scattering direction $\hat{\mathbf{r}}(\theta, \varphi)$. The cross-product term in eq 7 becomes $(\hat{\mathbf{r}} \times \mathbf{p}_{\text{eff}}) \times \hat{\mathbf{r}} = p_{\text{eff},\theta} \hat{\boldsymbol{\theta}} + p_{\text{eff},\varphi} \hat{\boldsymbol{\varphi}}$, and thus, eq 7 may be expressed as $\mathbf{E}^{(2\omega)} = E_{\theta}^{(2\omega)} \hat{\boldsymbol{\theta}} + E_{\varphi}^{(2\omega)} \hat{\boldsymbol{\varphi}}$ where the field components $E_{\theta}^{(2\omega)}(\theta, \varphi)$ and $E_{\varphi}^{(2\omega)}(\theta, \varphi)$ correspond to the parallel and perpendicular components of the SH field with respect to the scattering plane. The details of the RGD calculations are found in the Supporting Information. The radiation patterns may then be defined by the function

$$\Psi(\theta, \varphi) = |p_{\text{eff},\theta}(\theta, \varphi)|^2 + |p_{\text{eff},\varphi}(\theta, \varphi)|^2 \quad (8)$$

To illustrate, we now consider the approximate experimental parameters used in ref 1: $n = 1.4$, $\lambda = 800$ nm, $a = 0.5$ μm ; there is only a single independent nonlinear optical element, that is, $\chi_{s,\perp\parallel\parallel}^{(2)} = \chi_{s,\parallel\perp\parallel}^{(2)}$ ($\chi_{s,\perp\perp\perp}^{(2)} \approx 0$), which arise directly from eqs 6a and 6b (also note, $\chi_{s,x'y'z'}^{(2)} = 0$). For the case of the fundamental-field polarization $\hat{\mathbf{e}}_0 = \hat{\mathbf{x}}$, Figure 3a,b exhibits the SH radiation patterns, given by $\Psi(\theta, \varphi)$ along the scattering planes that are parallel and perpendicular to the incident light polarization, respectively. Figure 3c is the three-dimensional plot of the SH scattering pattern using the parameters above. This distinctive SH radiation pattern, as demonstrated in previous studies,⁹ is a consequence of the coherence of the SH sources from the surface of the sphere. Note from the figure that despite the vanishing signal in the axial direction, most of the SH radiation pattern is directed toward the forward direction, which can be captured by a large-numerical-aperture lens. In addition, the measurement of the SH intensity I_{SH} may be carried out in an angle-resolved or angle-integrated fashion since the Φ -dependence of the signal is independent of its direction $\hat{\mathbf{r}}$ because of the relation $I_{\text{SH}} \propto |\chi_{s,\perp\parallel\parallel}^{(2)}|^2 = |\chi_{s,\parallel\perp\parallel}^{(2)}|^2 \propto 1 + \cos \Phi$.

Before we conclude this section, we would like to discuss the nature of the coherence of the generated SH signal. For an individual particle, the total SH field is a coherent sum of all the fields generated by the individual dipole sources, that is, in our case, the molecular pairs, which are distributed throughout the surface of the sphere. This coherent summation takes into account the spatially dependent phases, amplitude, and direction of both input and SH fields at any given source point, and thus it governs the directional and polarization properties of the radiated SH field. A consequence of this coherence property is that the SH field in eq 7 is proportional to the nonlinear susceptibility elements, and hence the density N_s of the adsorbates or the dipole sources according to eq 4. Thus, to test if the SH signal is coherently generated, the SH signal I_{sph} from an individual sphere should scale quadratically with N_s , that is, $I_{\text{sph}} \propto N_s^2$. The quadratic dependence of the SH signal on the adsorbate density was first experimentally observed by Wang et al., thereby confirming the coherence of the SH signal arising from the surface of a sphere.⁶

When considering the total signal arising from N_p illuminated spheres generating the SH signal, on the other hand, the total SH signal may be written as⁸

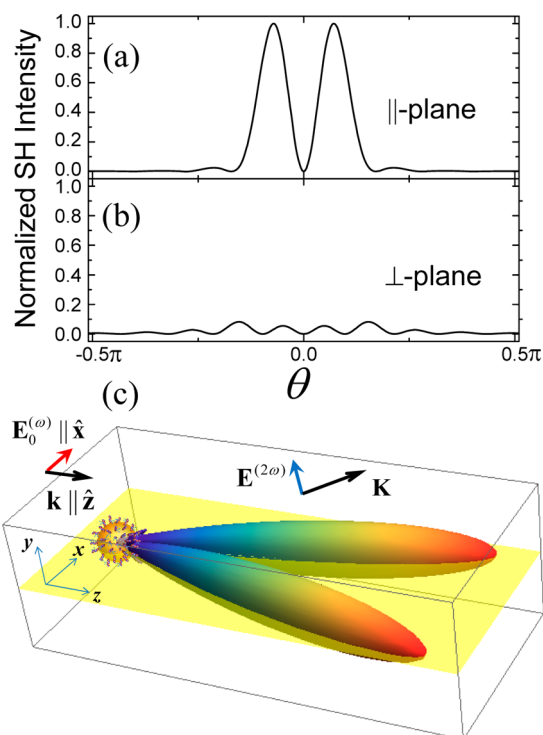


Figure 3. Normalized, angle-resolved SH radiation patterns collected along scattering planes (a) parallel and (b) perpendicular to the incident polarization (xz and yz planes, respectively) for the case of $n = 1.4$, $\lambda = 800$ nm, $a = 0.5$ μm , and $\mathbf{E}_0^{(\omega)} = E_0^{(\omega)}\hat{\mathbf{x}}$, with $\chi_{s,\perp\perp\perp}^{(2)} = 0$, $\chi_{s,\perp\parallel\parallel}^{(2)} = \chi_{s,\parallel\perp\perp}^{(2)} \neq 0$, and $\chi_{s,\perp\perp\parallel}^{(2)} = 0$. Note, for simplicity, the signals corresponding to the positive and negative θ values are given by $\Psi(\theta, \varphi)$ and $\Psi(|\theta|, \varphi + \pi)$, respectively, where $\Psi(\theta, \varphi)$ is defined in eq 8. (c) Three-dimensional plot of the SH radiation pattern. The quantities \mathbf{k} and \mathbf{K} denote the fundamental and SH wave vectors. Note that most of the SHG signal is contained within a half-cone angle of 30° in the forward direction.

$$I_{\text{SH}} \propto \left| \sum_{j=1}^{N_p} \mathbf{E}_j^{(2\omega)} e^{i\phi_j} \right|^2 = \sum_{j=1}^{N_p} |\mathbf{E}_j^{(2\omega)}|^2 + 2 \sum_{j \neq k}^{N_p} \text{Re} \{ \mathbf{E}_j^{(2\omega)} \cdot \mathbf{E}_k^{(2\omega)*} e^{i(\phi_j - \phi_k)} \} \quad (9)$$

where $\mathbf{E}_j^{(2\omega)}$ is the SH field arising from the j th sphere. For a sufficiently dilute concentration of spheres and if their relative phases are random, arising from the incoherent interference from the different particles, the second term in eq 9 vanishes, hence, $I_{\text{SH}} = N_p I_{\text{sph}}$, that is, the total SH intensity is a sum of the SH intensities from the individual particles. Thus, the nonlinear scattering process can be described as a single-particle scattering process.

OTHER THEORETICAL CONSIDERATIONS

Background Contribution to SH Signal. We now consider the contribution of background sources to the SH signal, which do not depend on the angle Φ . There are two types of background contribution: those arising from coherent sources (e.g., water polarization by the charged surface¹⁹ and other possible weak, nonresonant signals, such as the intrinsic chiral SHG from DNA and surface-generated signals) and those from incoherent sources (e.g., hyper-Rayleigh scattering²⁰). For a given SH radiation direction, $\hat{\mathbf{r}}(\theta, \varphi)$, where the SHG signal is

collected, the SH intensity may be written as $I_{\text{SH}} = I_{\text{inc}} + I_{\text{coh}}$, where I_{inc} and I_{coh} are the incoherent and coherent contributions to the SH signal, respectively. The term I_{coh} may be written as $I_{\text{coh}} = |E_{\text{coh}} e^{i\Delta} + E_{\Phi} \cos(\Phi/2)|^2$, where E_{coh} and E_{Φ} are parameters associated with the field amplitudes and Δ is the relative phase between the coherent background and the Φ -dependent terms.

In typical experiments, the incoherent contribution may be readily subtracted thus leaving only the coherent contribution. Let us consider this term for two special cases: $\Delta = 0$ and $\pi/2$. For $\Delta = 0$, that is, the coherent background term is in phase with the Φ -dependent signal, I_{coh} may be expressed as $I_{\text{coh}} = I_1 + I_2 \cos(\Phi/2) + I_3 \cos \Phi$, where I_1 , I_2 , and I_3 are constant parameters. Thus, for sufficiently small in-phase background contribution, the interference peaks associated with the $\cos \Phi$ term are still present but are now modulated according to the term $\cos(\Phi/2)$. When the two sources have a quadrature-phase relationship, that is, for the case of $\Delta = \pi/2$, I_{coh} may be expressed as $I_{\text{coh}} = I_1 + I_3 \cos \Phi = I_1(1 + g' \cos \Phi)$, where $g' = I_3/I_1$. As an example of a system in which the two coherent contributions are in quadrature phase, the background may arise from the nonresonant polarization of the water molecules due to the strong surface charge from the adsorbed DNA molecules on the surface of the particle, whereas the Φ -dependent term arises from the two-photon resonant SHG from the daunomycin molecules. The nonresonant polarization component may be included directly in the calculation of $\mathbf{E}^{(2\omega)}(\mathbf{r})$ in eq 7 with the replacement $\chi_{s,\perp\perp\perp}^{(2)} \rightarrow \chi_{s,\perp\perp\perp}^{(3)} V_0$, where $\chi_{s,\perp\perp\perp}^{(3)}$ is the bulk third-order nonlinear susceptibility and V_0 is the electric potential at the surface of the particle, which is associated with the polarization of the water molecules.¹⁹

Another possible scenario is the case in which $E_{\text{coh}} \approx 0$. Thus, the total SH signal at a certain detector position is given by $I_{\text{SH}} = I_0(1 + g \cos \Phi)$, where the parameters I_0 and g are given by $I_0 = I_{\text{inc}} + (1/2)|E_{\Phi}|^2$ and $g = |E_{\Phi}|^2/(|E_{\Phi}|^2 + 2I_{\text{inc}})$. As a consequence, the modulation depth of SH interference signal decreases due to increasing incoherent-background contribution. This is likely the case observed in ref 1, and thus, the actual SH signal dependence with base-pair separation possesses both modulating and nonmodulating components, in agreement with our derived $(1 + g \cos \Phi)$ -dependence of the SH signal.

Probing Binding-Induced Change in DNA Structure.

The sensitivity of SHG to structural changes has been established in earlier experiments on the binding of the restriction enzyme EcoR1 to its recognition site on a 90mer DNA duplex.²¹ It was manifested by a rapid and large increase in the SH intensity upon addition of EcoR1 to the solution containing DNA. This increase was attributed to the enzyme inducing the known change in the DNA structure transforming it from its normal rod-like conformation to a bent conformation. By not including the Mg^{2+} cofactor in the DNA solution, the SHG signal obtained when EcoR1 is added to the solution indicates that although there is binding of EcoR1 and bending of DNA, there is no cleavage of DNA. Using the SH interference method, we have the capability to differentiate winding from the unwinding of a DNA duplex by a relatively simple change in the interference pattern, which can be described as follows: A modulated reference pattern is obtained in the measurements of the SH intensity as the number of base pairs separating the two bound daunomycin molecules is increased or decreased. As discussed above, a translation of daunomycin by a single base pair, up or down the

helix, imparts a rotation of 36° for daunomycin with respect to the helical axis. Thus, the number of base pairs separating the daunomycin molecules determines their relative orientation.

The recognition site of the binding drug, protein, and so on, is placed between the two daunomycin molecules constituting the molecular pair. The nature of the perturbation effected by the binding of a foreign molecule to DNA determines whether there is increased winding, unwinding, or bending of the DNA helix. As an example, the antiviral and antibiotic drug netropsin complexes with DNA by minor groove binding, which results in an increased winding of the DNA helix.^{22–24} With the interference method, the increased winding would be manifested by a shift and higher frequency interference pattern with respect to the interference pattern of the reference sample, that is, the pattern obtained without netropsin. The introduction of netropsin leads to an increase in the twist per base pair, which would result in the modulation in the SH signal occurring at a smaller number of base pairs separating the daunomycin molecules, as illustrated in Figure 4. For the case

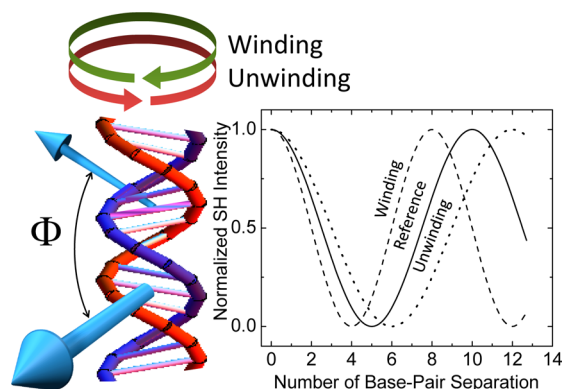


Figure 4. Effect of increasing (winding) or decreasing (unwinding) the DNA helical twist per base pair on the SH signal as a function of base-pair separation. Increasing (decreasing) the twist per base pair would result in the modulation in the SH signal occurring at a smaller (larger) number of base pairs separating the daunomycin molecules relative to a reference configuration.

when unwinding is the result of a foreign molecule binding to DNA, the shift in the interference pattern would be in the opposite direction, that is, toward an increased number of base pairs separating the daunomycin molecules. In addition to information on the structural change in DNA, that is, winding versus unwinding, the magnitude of the shift would indicate the change in the twist angle of the DNA helix.

SUMMARY AND OUTLOOK

We have calculated the SH electric field and radiation patterns for an aqueous solution containing DNA duplexes affixed to a 1 μm dielectric sphere, where each duplex contains an intercalated pair of SH-active chromophores. The model that we have developed predicts that the SH intensity generated by a solution of such particles would yield an interference pattern that oscillates with a frequency determined by the number of base pairs separating the two chromophores, a prediction that is in excellent agreement with our experimental findings.

The binding of a molecule, for example, a protein or drug, to a recognition site located between the two chromophores, would typically induce a change in the structure of DNA by a winding, unwinding, or bending of the DNA duplex. The

alteration of the DNA structure would cause a change in the separation of the SH chromophores, which would thereby change their relative orientation and, as a consequence, the SH interference pattern. This interference method has the potential of providing a new way to probe structural changes in DNA induced by a perturbation such as the formation of DNA–biomolecule complexes. Furthermore, this interference method can be used to observe the dynamics of conformational motions of macromolecules at aqueous interfaces.

ASSOCIATED CONTENT

Supporting Information

Calculation of SH nonlinear susceptibility tensor elements for a surface with isotropic symmetry. Calculation of the SH field under the RGD approximation for a spherical particle. This material is available free of charge via the Internet at <http://pubs.acs.org>.

AUTHOR INFORMATION

Corresponding Author

*E-mail: dadap.cumsl@gmail.com.

Notes

The authors declare no competing financial interest.

ACKNOWLEDGMENTS

The authors would like to acknowledge useful conversations with Tony Heinz and Yi Rao. One of the authors (K.B.E.) would like to acknowledge funding from the NSF Eager Award CHE-1041980, NSF CHE-1057483, and DTRA HDTRA1-11-1-0002.

REFERENCES

- (1) Doughty, B.; Rao, Y.; Kazer, S. W.; Kwok, S. J. J.; Turro, N. J.; Eisenthal, K. B. Probing the Relative Orientation of Molecules Bound to DNA through Controlled Interference Using Second-Harmonic Generation. *Proc. Natl. Acad. Sci. U.S.A.* **2013**, *110*, 5756–5758.
- (2) Chaires, J. B.; Fox, K. R.; Herrera, J. E.; Britt, M.; Waring, M. J. Site and Sequence Specificity of the Daunomycin–DNA Interaction. *Biochemistry* **1987**, *26*, 8227–8236.
- (3) Moore, M. H.; Hunter, W. N.; d'Estaintot, B. L.; Kennard, O. DNA–Drug Interactions. The Crystal Structure of d(CGATCG) Complexed with Daunomycin. *J. Mol. Biol.* **1989**, *206*, 693–705.
- (4) Leslie, A. G. W.; Amott, S.; Chandrasekaran, R.; Ratliff, R. L. Polymorphism of DNA Double Helices. *J. Mol. Biol.* **1980**, *143*, 49–72.
- (5) Heinz, T. F. Second-Order Nonlinear Optical Effects at Surfaces and Interfaces. In *Nonlinear Surface Electromagnetic Phenomena*; Ponath, H., Stegeman, G., Eds.; Elsevier: Amsterdam, 1991; pp 353–416.
- (6) Wang, H.; Yan, E. C. Y.; Borguet, E.; Eisenthal, K. B. Second Harmonic Generation from the Surface of Centrosymmetric Particles in Bulk Solution. *Chem. Phys. Lett.* **1996**, *259*, 15–20.
- (7) Dadap, J. I.; Shan, J.; Eisenthal, K. B.; Heinz, T. F. Second-Harmonic Rayleigh Scattering from a Sphere of Centrosymmetric Material. *Phys. Rev. Lett.* **1999**, *83*, 4045.
- (8) Eisenthal, K. B. Second Harmonic Spectroscopy of Aqueous Nano- and Microparticle Interfaces. *Chem. Rev.* **2006**, *106*, 1462–1477.
- (9) Roke, S.; Gonella, G. Nonlinear Light Scattering and Spectroscopy of Particles and Droplets in Liquids. *Annu. Rev. Phys. Chem.* **2012**, *63*, 353–378.
- (10) Martorell, J.; Vilaseca, R.; Corbalan, R. Scattering of Second-Harmonic Light from Small Spherical Particles Ordered in a Crystalline Lattice. *Phys. Rev. A* **1997**, *55*, 4520–4525.

- (11) Yang, N.; Angerer, W. E.; Yodh, A. G. Angle-Resolved Second-Harmonic Light Scattering from Colloidal Particles. *Phys. Rev. Lett.* **2001**, *87*, 103902.
- (12) Roke, S.; Roeterdink, W. G.; Wijnhoven, J. E. G. J.; Petukhov, A. V.; Kleyn, A. W.; Bonn, M. Vibrational Sum Frequency Scattering from a Submicron Suspension. *Phys. Rev. Lett.* **2003**, *91*, 258302.
- (13) Dadap, J. I.; Shan, J.; Heinz, T. F. Theory of Optical Second-Harmonic Generation from a Sphere of Centrosymmetric Material: Small-Particle Limit. *J. Opt. Soc. Am. B* **2004**, *21*, 1328–1348.
- (14) de Beer, A. G. F.; Roke, S. Sum Frequency Generation Scattering from the Interface of an Isotropic Particle: Geometrical and Chiral Effects. *Phys. Rev. B* **2007**, *75*, 245438.
- (15) Dadap, J. I. Optical Second-Harmonic Scattering from Cylindrical Particles. *Phys. Rev. B* **2008**, *78*, 205322.
- (16) Jen, S.-H.; Dai, H.-L.; Gonella, G. The Effect of Particle Size in Second Harmonic Generation from the Surface of Spherical Colloidal Particles. II: The Nonlinear Rayleigh-Gans-Debye Model. *J. Phys. Chem. C* **2010**, *114*, 4302–4308.
- (17) Viarbitskaya, S.; Kapshai, V.; van der Meulen, P.; Hansson, T. Size Dependence of Second-Harmonic Generation at the Surface of Microspheres. *Phys. Rev. A* **2010**, *81*, 53850.
- (18) de Beer, A. G. F.; Roke, S.; Dadap, J. I. Theory of Optical Second-Harmonic and Sum-Frequency Scattering from Arbitrarily Shaped Particles. *J. Opt. Soc. Am. B* **2011**, *28*, 1374–1384.
- (19) Ong, S.; Zhao, X.; Eiseenthal, K. B. Polarization of Water Molecules at a Charged Interface: Second Harmonic Studies of the Silica/Water Interface. *Chem. Phys. Lett.* **1992**, *191*, 327–335.
- (20) Terhune, R. W.; Maker, P. D.; Savage, C. M. Measurements of Nonlinear Light Scattering. *Phys. Rev. Lett.* **1965**, *14*, 681–684.
- (21) Doughty, B.; Kazer, S. W.; Eiseenthal, K. B. Binding and Cleavage of DNA with the Restriction Enzyme EcoRI Using Time-Resolved Second Harmonic Generation. *Proc. Natl. Acad. Sci. U.S.A.* **2011**, *108*, 19979–19984.
- (22) Lipfert, J.; Klijnhout, S.; Dekker, N. H. Torsional Sensing of Small-Molecule Binding Using Magnetic Tweezers. *Nucleic Acids Res.* **2010**, *38*, 7122–7132.
- (23) Triebel, H.; Bär, H.; Walter, A.; Burckhardt, G.; Zimmer, C. Modulation of DNA Supercoiling by Interaction with Netropsin and Other Minor Groove Binders. *J. Biomol. Struct. Dyn.* **1994**, *11*, 1085–1105.
- (24) Snounou, G.; Malcolm, A. D. B. Production of Positively Supercoiled DNA by Netropsin. *J. Mol. Biol.* **1983**, *167*, 211–216.